HYBRID DISTRIBUTED GENERATION SYSTEMS USING A DC MICROGRID

[1]M.SAI LAKSHMI, [2]K.DAYAKAR

[1]PG Scholar, [2]Associate Professor, Department of EEE,

[1,2]Geethanjali Institute of Science and Technology, affiliated to JNTUA, Gangavaram, SPSR Nellore.

ABSTRACT

Keeping in mind the end goal to think about the vulnerability and irregular attributes of wind power and wave power, this paper proposes a coordinated breeze and wave power age framework nourished to an air conditioner power matrix or associated with a separated load utilizing a dc microgrid. The proposed dc microgrid interfaces with a breeze power generator through a voltage-source converter (VSC), a wave power generator through a VSC, an energy stockpiling battery through a bidirectional dc/dc converter, a resistive dc stack through a heap dc/dc converter, and an air conditioner power framework through a bidirectional network tied inverter.

The concentrated coordinated breeze and wave framework joined with the dc microgrid is demonstrated and mimicked utilizing the composed program in light of MATLAB/Simulink. Root-loci plots of the examined framework under different rates of the wave generator are investigated. To look at the central working qualities of the concentrated coordinated framework joined with the dc microgrid, a lab scale stage is likewise settled. Relative recreation and trial comes about uncover that the concentrated incorporated framework can keep up stable operation to supply power under various working conditions utilizing the proposed dc microgrid.

I. INTRODUCTION

As of late, renewable energy and conveyed age frameworks (DGSs) have pulled in expanding consideration and have been broadly inquired about and created. They continuously modify the ideas and operations of ordinary power age frameworks. The ascent in a few nations makes it conceivable that this sort of DGS can be for all intents and purposes connected to a framework tied framework or a disengaged framework with wind power, sun oriented energy, hydropower, and so forth. The yield of DGS ordinarily incorporates two sorts: dc and variable air conditioning. In addition, the producing limit of DGS contrasting and customary substantial synchronous generators is significantly littler, and henceforth, the dc microgrid can be essentially connected to change over the created time-differing amounts of common renewable energy and DGS into smooth dc electricity that would then be able to be changed over again into air conditioning amounts conveyed to other power frameworks [1], [2]. In light of the discontinuity of renewable energy and DGS, bidirectional dc/dc converters are generally important to bolster the associated loads with smooth power [3].

Unexplored energy and resources in sea, for example, marine energy, tidal energy, sea warm energy, sea wave energy, saltiness angle energy, and so forth., are bounteous. The reproduced consequences of an Archimedes wave swing (AWS) power convertor coupling with a direct changeless magnet generator (LPMG) were contrasted and the test results utilizing the deliberate information got from a 2-MW AWS test framework along the coastline [6]. A design of a marine power plant with two AWSs associating with a power network was proposed in [7], and the yields of the two AWSs were changed over to dc amount by singular diode connect rectifiers and after that along these lines changed over into air conditioning amount by an inverter to lessen the vacillation of the joined corrected yield power. A mixture electric vehicular power framework in [8] used two engines associated with a dc transport through a voltage-source converter (VSC), and a bidirectional converter was associated between a battery and the dc transport. The dynamic normal model was utilized as a part of [8] for all power

hardware models by disregarding the changing wonders to decrease reenactment computational force.

A nonisolated bidirectional zero-voltage exchanging dc/dc converter was proposed in [9], and the converter used an extremely basic helper circuit comprising of an extra twisting of a principle inductor and an assistant inductor to achieve zero voltage exchanging and diminish the invert recuperation issue of power diodes. Displaying and testing the server farms of a dc microgrid utilizing PSCAD/EMTDC were proposed in [10] and since most server farms were touchy to the varieties of electronic burdens. The proposed dc microgrid was likewise used to supply touchy electronic burdens amid air conditioning framework blackouts so as to offer uninterruptible power framework security . A 12-kW trial framework was built in [to affirm the adequacy of the proposed plot. To accomplish power sharing and to upgrade the dc microgrid, the control techniques for an islanded microgrid with a dc-interface voltage control were produced , while the control procedures were joined with P/V hang control and consistent power band to stay away from visit changes and voltage-restrain infringement on age gadgets. A battery/ultra capacitor cross breed energy stockpiling framework was proposed in for electric-drive vehicles. To fulfill the pinnacle power requests between the ultra capacitor and battery, a bigger dc/dc converter was important. The examined framework used two stockpiling gadgets to repay commonly keeping in mind the end goal to draw out the life of the battery. The reenacted and test comes about were completed to confirm the proposed control framework .

This paper proposes an incorporated breeze and wave power age framework sustained to a power framework or associated with a detached load utilizing a dc microgrid. A bidirectional dc/dc converter is proposed to accomplish the joining of both breeze and wave power age frameworks with vulnerability and discontinuous attributes. This paper is sorted out as takes after. Segment II presents the framework arrangement and utilized models. Segment III delineates the framework design of the research facility review coordinated breeze and wave power age framework. Root-loci plots of the concentrated coordinated framework under different velocities of AWS are appeared in Section IV to inspect the stability of the contemplated framework. Similar mimicked and exploratory aftereffects of the examined framework under a sudden load exchanging condition are exhibited in Section V. The particular vital finish of this paper is attracted Section VI.

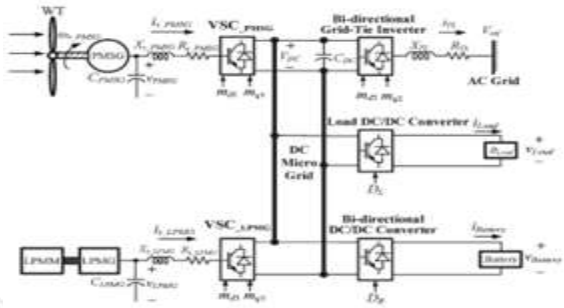

Fig. 1. Configuration of the studied integrated wind and wave power generation system connected to a power grid through the proposed dc microgrid.

II. CONFIGURATION OF THE STUDIED SYSTEM

A. System Configuration

Fig. 1 demonstrates the setup of the concentrated integrated breeze and wave power age framework associated with an air conditioner lattice through a dc microgrid. The breeze power age framework reproduced by a perpetual magnet synchronous generator (PMSG) driven by a breeze turbine (WT) is associated with the dc microgrid.

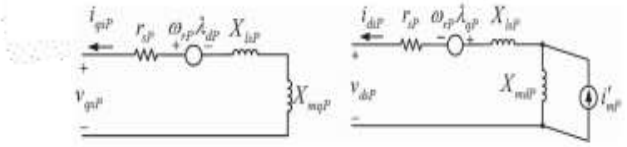

Fig. 2. q–d-axis equivalent circuit model of the studied wind PMSG.

through a VSC of VSC_PMSG. The wave power age framework mimicked by a LPMG driven by a direct perpetual magnet engine (LPMM) is additionally associated with the dc microgrid through a VSC of VSC_LPMG. A resistive dc stack RLoad is associated with the dc microgrid through a heap dc/dc converter. To accomplish stable power stream (or power adjust condition) and load request

control of the dc microgrid under various working conditions, a battery is associated with the dc microgrid through a bidirectional dc/dc converter, while an air conditioner network is associated with the dc microgrid through a bidirectional matrix tied inverter and a transmission line. At the point when accessible breeze power or potentially wave power can be infused into the dc microgrid with a completely charged battery, the surplus power of the dc microgrid can be conveyed to the air conditioner framework through the bidirectional lattice tied inverter.

At the point when no breeze power or no wave power is conveyed to the dc microgrid with a low-energy battery, the inadequate power of the dc microgrid can be caught from the air conditioner matrix through the bidirectional lattice tied inverter. The power of the resistive dc stack RLoad can be acquired from the dc microgrid through the heap dc/dc converter just when the dc microgrid has enough power. The heap dc/dc converter with the resistive dc stack RLoad can likewise somewhat alter the power adjust state of the dc microgrid.

The control elements of the bidirectional dc/dc converter, the bidirectional matrix tied inverter, and the heap dc/dc converter must be satisfactorily organized with each other to get steady operation of the dc microgrid. In this paper, the scientific models of the concentrated integrated framework with the proposed dc microgrid are inferred in detail, including the breeze WT-PMSG set with its VSC, the wave LPMM-LPMG set with its VSC, the bidirectional dc/dc converter with the battery, the heap dc/dc converter with the resistive load, and the bidirectional network tied inverter. Both recurrence space examination and time-area reproductions are performed utilizing MATLAB/Simulink.

B.Models of WT and PMSG

The WT demonstrate utilized in this paper incorporates the accompanying operation conditions: the cut-in twist speed of 4 m/s, the evaluated twist speed of 13 m/s, and the cut-out breeze speed of 24 m/s. The definite qualities and articulations for the caught mechanical power Pw, the dimensionless power coefficient Cpw, the mechanical torque Tw, the tip speed proportion λw, and the cutting edge pitch point βw of the examined WT can be seen in . Fig. 2 plots the q– d-pivot equal circuit of the examined wind PMSG . The per-unit (p.u.) q-and d-pivot stator winding voltages of the contemplated PMSG can be communicated by, separately,

$$v_{qsP} = -r_{sP} i_{qsP} + p(\lambda_{qP})/\omega_b + \omega_{rP}\lambda_{dP}/\omega_b \quad (1)$$

$$\text{illegible} \quad (2)$$

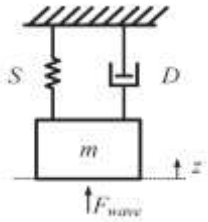

Fig. 3. Equivalent mass-spring-damper model of the studied AWS.

Where,

$$\lambda_{qP} = -(X_{mqP} + X_{lsP}) i_{qsP} \quad (3)$$

$$\lambda_{dP} = -(X_{mdP} + X_{lsP}) i_{dsP} + X_{mdP} i'_{mP} \quad (4)$$

are the q- and d-axis stator-winding magnetic fluxes, respectively; *iqsP* and *idsP* are the q- and d-axis stator-winding currents, respectively; X_{mqP} and X_{mdP} are the q- and d-axis magnetizing reactances, respectively; X^{l}_{sP} is the leakage reactance; i mP is the magnetizing current; r_{sP} is the stator winding equivalent resistance; and ω_{rP} is the rotor speed of the studied PMSG, while p is the differential operator with respect to time t (i.e., p = d/dt), and ω_b is the base angular speed in radians per second.

C.Models of AWS and LPMG

The AWS uses the wave swing to drive the generator to deliver electric power without transmission medium. The movement of the AWS in liquid is influenced by the damping power and spring power. The comparable mass-spring-damper model of the considered AWS is represented in Fig. 3, whose movement conditions can be portrayed by

$$p(z) = u \quad (5)$$

$$(m)p(u) = F_{\text{wave}} - (S)z - (D)u \quad (6)$$

where m is the total of the majority of the floater and the LPMG translator; D and S are the damping coefficient and spring steady, individually; and F wave, z, and u are the floater main impetus, remove went by the floater, and speed of the floater of the AWS, separately. Fig. 4 draws the q– d-hub equal circuit model of a LPMG. The nonlinear p.u.

differential conditions of the LPMG can be composed as

$$(X_q)p(i_{qsg}) = -v_{qsg} - Ku_s X_{mdg} i_{qsg} - R_{sg} i_{qsg} + Ku_s X_{mdg} i'_{mg} \quad (7)$$

$$(X_d)p(i_{dsg}) = -v_{dsg} + Ku_s X_{mqg} i_{qsg} - R_{sg} i_{dsg} \quad (8)$$

where idsg and iqsg are the d-and q-hub equal magnetizing currents, individually; I mg is the magnetizing current; Xlsg is the proportionate spillage reactance; Rsg is the equal interior protection; Xmqd and Xmdg are the q-and d-pivot magnetizing inductance, separately; and Xd = Xlsg + Xmdg and Xq = Xlsg + Xmqg of the examined LPMG, while K = π/τp, τp is the cathode separation, and us is the forcer development speed of the LPMG.

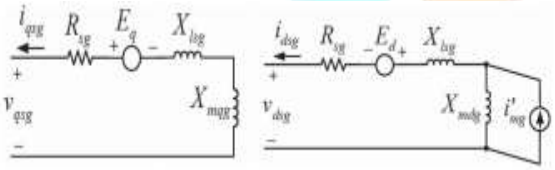

Fig. 4. q–d-axis equivalent circuit model of the studied LPMG.

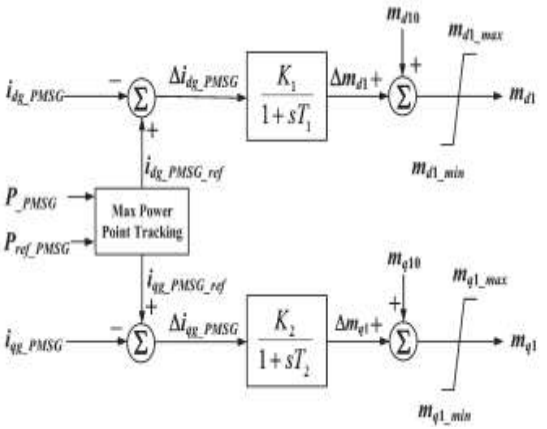

Fig. 5. Control block diagram of the modulation indices of the VSC of the studied PMSG.

D.Control Blocks of PMSG's VSC

Fig. 5 outlines the control square graphs of the lists mq1 and md1 of the concentrated PMSG's VSC. The d-and q-hub reference currents are produced by looking at the yield dynamic power of the PMSG (PPMSG) with its reference esteem utilizing most extreme power point following capacity. In the wake of subtracting the yield currents of the PMSG (ig_PMSG) from their particular reference esteems, the resultant contrasts go through the individual first-arrange slack controllers to get the deviations of the separate tweak files that are added to their separate beginning esteems to gain the VSC's adjustment files. The limiters, in particular, md1_ max, md1_ min, mq1_ max, and mq1_ min, are incorporated into the model to guarantee typical operation of the VSC.

E.Control Blocks of LMSG's VSC

Fig. 6 plots the control piece graphs of the lists mq3 and md3 of the concentrated LPMG's VSC. In the wake of subtracting the yield currents of the LPMG (ig_LMSG) from their individual reference esteems, the resultant contrasts go through the separate corresponding necessary controllers to get the deviations of the particular regulation files which are added to their separate introductory esteems to get the VSC's tweak records. The limiters, specifically, md3_ max, md3_ min, mq3_ max, and mq3_ min, are incorporated into the model to guarantee ordinary operation of the VSC.

F.Control Blocks of Bidirectional Grid-Tied Inverter

Fig. 7 draws the control square chart of the balance records mq2 and md2 of the lattice tied voltage-source inverter (VSI). The lattice fixing VSI is required to nourish the produced power of the renewable-energy frameworks to the power matrix to consent to the network side electrical amounts, for example, voltage greatness, stage succession, stage point, recurrence, and so on. The principle control point of the VSI is to settle the dc-transport voltage by modifying the dynamic power of the dc microgrid conveyed to or acquired from the air conditioner matrix. Subsequent to subtracting the dc-transport voltage (VDC), the terminal voltage of the VSI (vINV), and the aggregate power of the dc

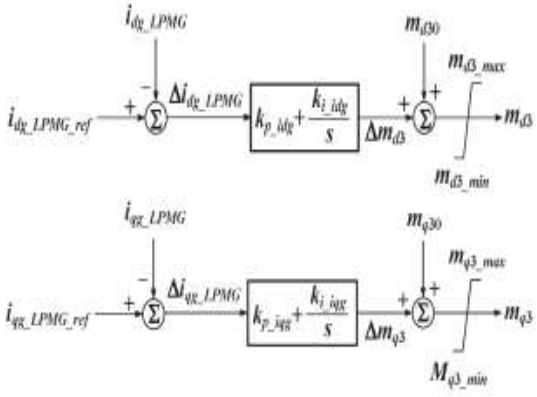

Fig. 6. Control block diagram of the modulation indices of the VSC of the studied LPMG.

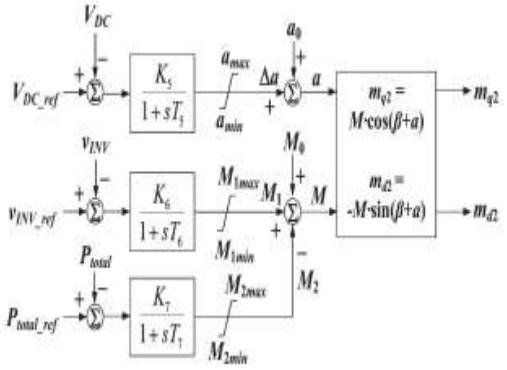

Fig. 7. Control block diagram of the modulation indices of the grid-tied VS.

microgrid (Ptotal) from the separate reference esteems, the individual contrasts go through firstorder slack controllers to get the deviations Δa, M1, and M2, separately. By including Δa, M1, and M2 to their individual introductory esteems, the dynamic power, terminal voltage, and stage edge at the yield terminals of the VSI can be gotten. On the off chance that the aggregate power of the dc microgrid is lower than the reference add up to power, the power of the dc microgrid is gotten from the air conditioner utility lattice to repay the heap request. On the off chance that the aggregate power of the dc microgrid is higher than the reference add up to power, the surplus power of the dc microgrid is sent to the air conditioner utility network to adjust the power of the dc microgrid. It is to guarantee that the utilized bidirectional network tied inverter can yield a steady air conditioning voltage nourished to the air conditioner lattice by keeping up stability of the dc microgrid

G.Model of Bidirectional DC/DC Converter

Fig. 8(a) demonstrates the fundamental schematic outline of the utilized bidirectional dc/dc converter with a synchronous-buck structure. The converter comprises of two power switches (S1 and S2) and an energy-store inductance LBattery. The plan reason for this converter is that the energy stockpiling inductance can be associated with either the dc transport of the dc microgrid or the battery on

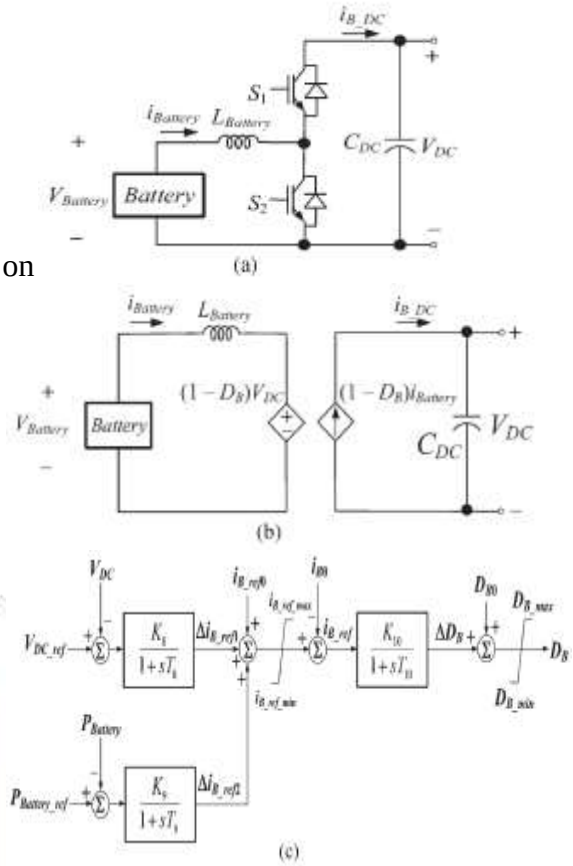

Fig.8. Essential schematic outline, dynamic normal esteem model, and control square graph of the utilized bidirectional dc/dc converter. (a) Basic schematic graph. (b) Dynamic normal esteem demonstrate. (c) Control piece chart. the low-voltage side.

The usage of the two power switches S1 and S2 can adequately accomplish lift or buck method of operation, while the heading of power stream between the dc microgrid and the battery can likewise be exchanged. The attributes of the bidirectional dc/dc converter are distinctive under lift or buck method of operation. The dynamic normal esteem display appeared in Fig. 8(b) is utilized as a part of this paper, where the exchanging components are supplanted by a reliant current source and a needy voltage source to set up another circuit.

Expect that the high-recurrence exchanging wonders are disregarded. To get both basic lift mode and buck method of control, high-recurrence pulsewidth tweak (PWM) must be ignored by applying obligation proportion control to accomplish bidirectional capacities as takes after: 1) support method of operation

$$L_{\text{Battery}}p(i_{\text{Battery}}) = V_{\text{Battery}} - (1 - D_B)V_{\text{DC}} - i_{\text{Battery}} \cdot R_{\text{Battery}} \quad (9)$$

$$i_{B\_DC} = C_{\text{DC}}p(V_{\text{DC}}) = (1 - D_B) \cdot i_{\text{Battery}} \quad (10)$$

2) buck mode of operation

$$L_{\text{Battery}}p(i_{\text{Battery}}) = D_B \cdot V_{\text{DC}} - V_{\text{Battery}} - i_{\text{Battery}} \cdot R_{\text{Battery}} \quad (11)$$

$$i_{B\_DC} = C_{\text{DC}}p(V_{\text{DC}}) = D_B \cdot i_{\text{Battery}} \quad (12)$$

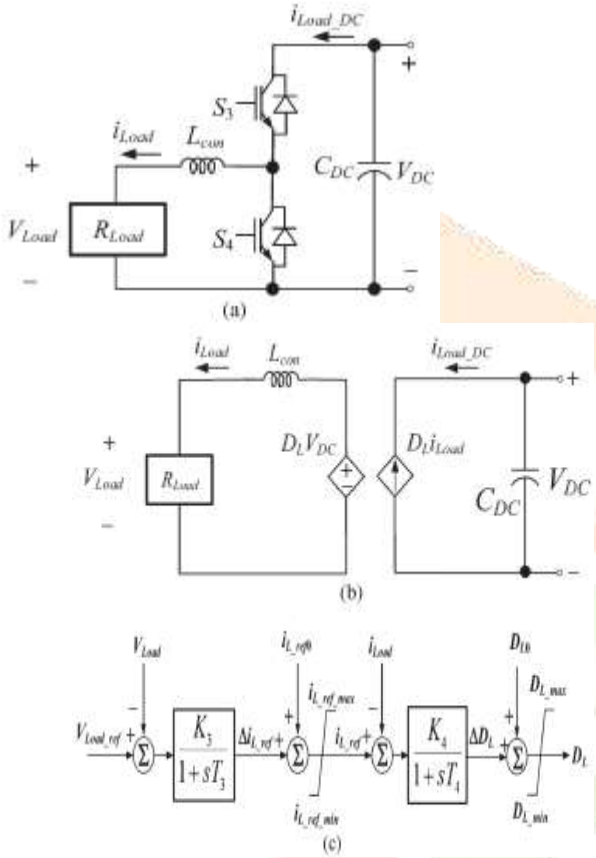

Fig.9. Basic schematic diagram, dynamic average-value model, and control block diagram of the employed load dc/dc converter. (a) Basic schematic diagram. (b) Dynamic average-value model. (c) Control block diagram.

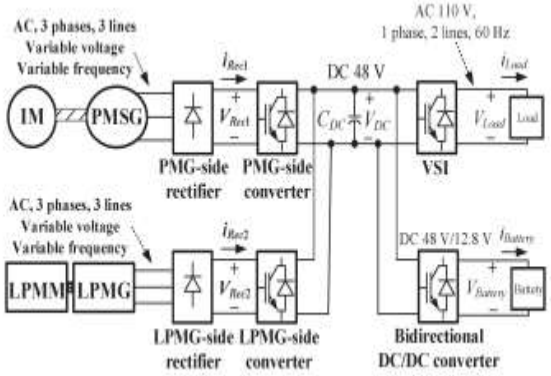

Fig.10. Configuration of the laboratory renewable-energy generation system.

where DB is the obligation proportion of the converter, CDC is the comparable capacitance of the dc microgrid, LBattery is the outer inductance of the battery, RBattery is the inward protection of the battery, and iBattery and iB_DC are the currents at the low voltage and high-voltage sides of the converter, separately.

So as to take care of the control issue of the bidirectional converter under two diverse power stream bearings, the control technique depends on an inward current circle control joined with an external voltage circle control. Fig. 8(c) demonstrates the two criticism circles for the battery charging power control and the dc voltage control of the dc microgrid. At the point when unsettling influences happen, the control of VDC can be accomplished by changing the battery charging current through nourishing back VDC and PBattery.

III.SIMULATED RESULTS

A simulation design system is implemented in MATLAB SIMULINK with the help of switches and voltage sources we get desired output voltage.

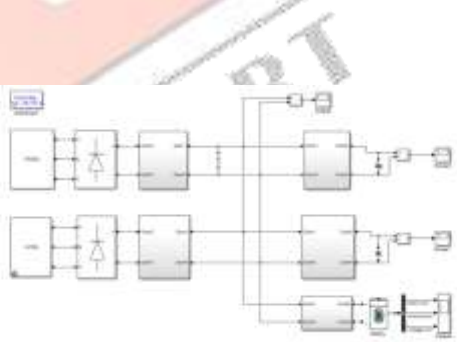

Fig.11:Circuit model

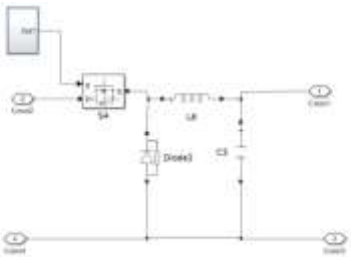

Fig.12:PMSG and LPMG side converter

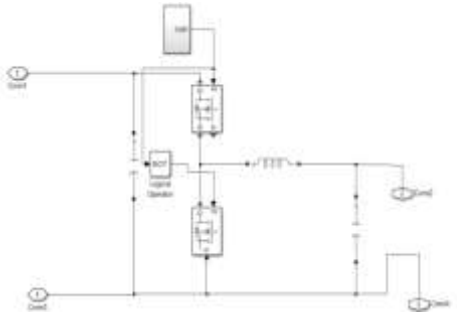

Fig.13:Bi-Directional dc-dc converter

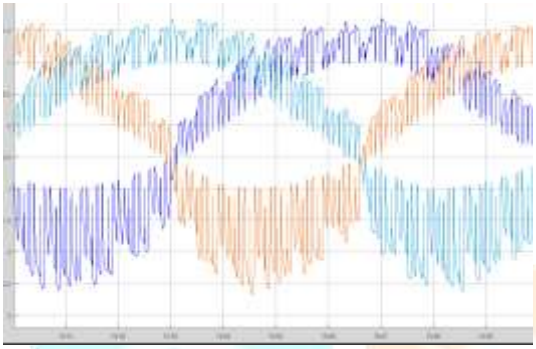

Fig.14:Output current of PMSG

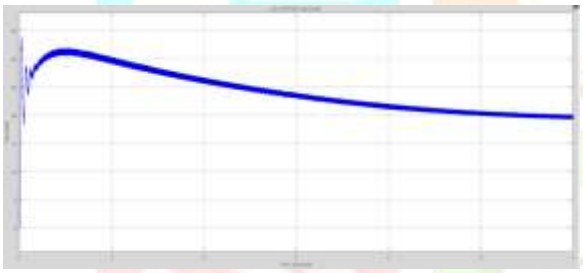

Fig.15:Dc output voltage waveform

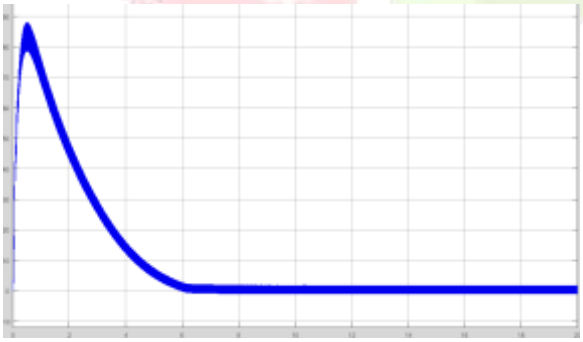

Fig.16:Dc output current waveform

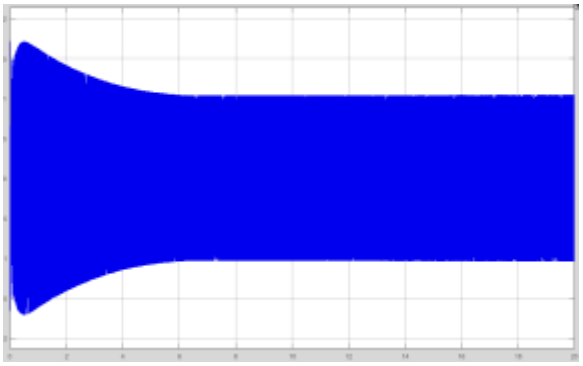

Fig.17:Dc/ac inverter output current

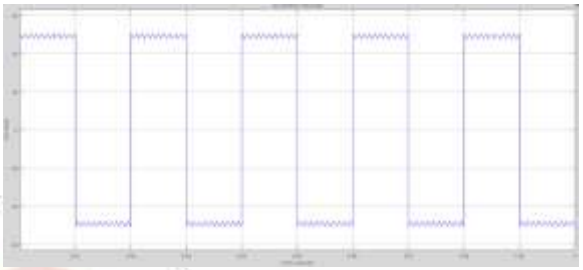

Fig.18:Ac output voltage waveform

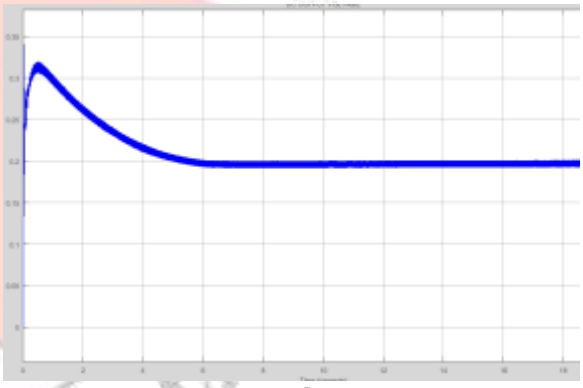

Fig.19:Load current

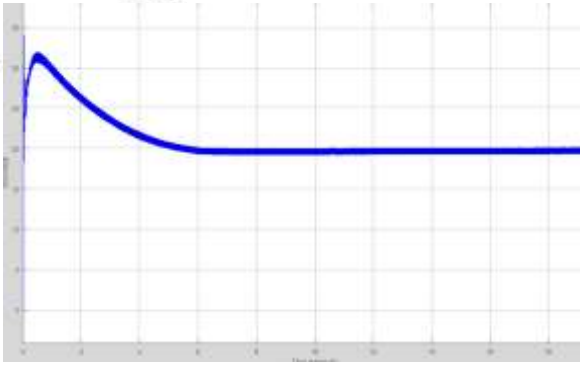

Fig.20:Load voltage

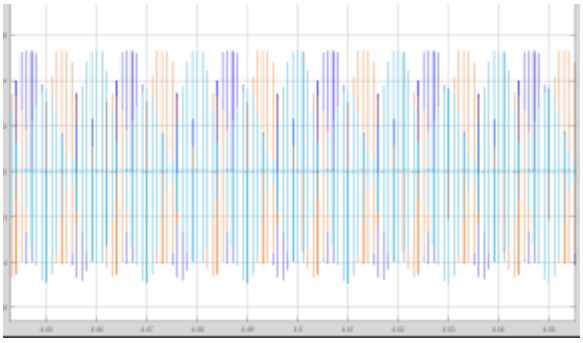

Fig.21:Output voltage of lpmg

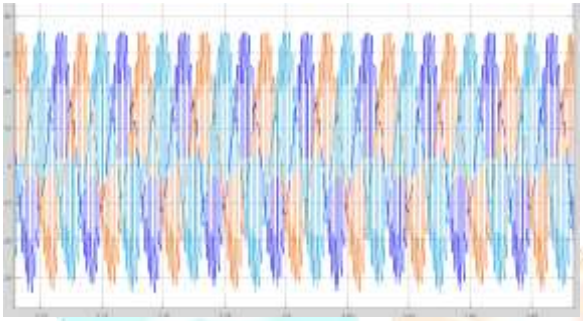

Fig.22:Output current of lpmg

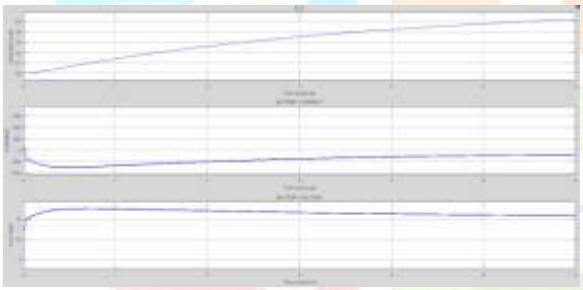

Fig.23:Battery waveform

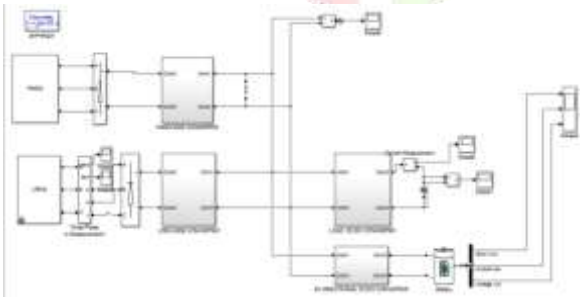

Fig.24:Extension simulation circuit

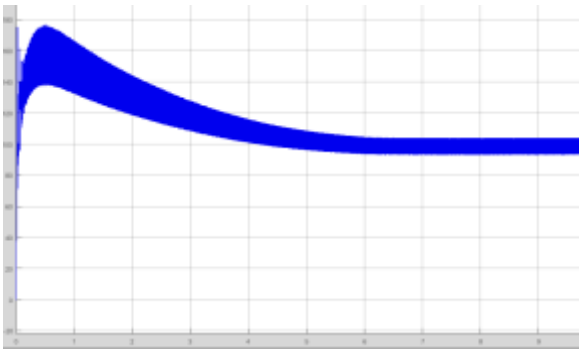

Fig.25:Dc output voltage waveform

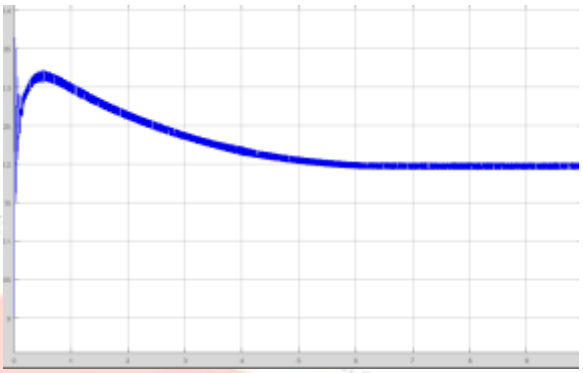

Fig.26:Output current

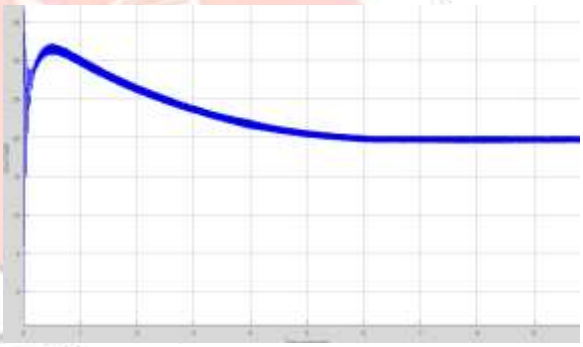

Fig.27:Output voltage

IV. CONCLUSION

An integration of both wind power and wave power age frameworks joined with a dc microgrid has been proposed. A research facility grade test framework has been exhibited in this paper to analyze the principal working qualities of the concentrated integrated framework sustained to secluded burdens utilizing a dc microgrid. For reproduction parts, the consequences of the root-loci plot and the time-area reactions have uncovered that the concentrated integrated framework with the proposed dc microgrid can keep up stable operation under a sudden load-switching condition.

Near reproduced and measured outcomes under a heap switching have been performed, and it demonstrates that the concentrated integrated framework with the proposed dc microgrid can be worked steadily under various unsettling influence conditions, while both measured and mimicked results can coordinate with each other.

REFERENCES

[1] Y. Ito, Y. Zhongqing, and H. Akagi, "DC microgrid based distribution power generation system," in Proc. 4th IEEE Int. Power Electron. Motion Control Conf., 2004, vol. 3, pp. 1740–1745.

[2] S. K. Kim, J. H. Jeon, C. H. Cho, J. B. Ahn, and S. H. Kwon, "Dynamic modeling and control of a grid-connected hybrid generation system with versatile power transfer," IEEE Trans. Ind. Electron., vol. 55, no. 4, pp. 1677–1688, Apr. 2008.

[3] C. Abbey and G. Joos, "Supercapacitor energy storage for wind energy applications," IEEE Trans. Ind. Appl., vol. 43, no. 3, pp. 769–776, May 2007.

[4] X. Liu, P. Wang, and P. C. Loh, "A hybrid ac/dc microgrid and its coordination control," IEEE Trans. Smart Grid, vol. 2, no. 2, pp. 278–286, Jun. 2011.

[5] H. Kakigano, Y. Miura, and T. Ise, "Low-voltage bipolar-type dc microgrid for super high quality distribution," IEEE Trans. Power Electron., vol. 25, no. 12, pp. 3066–3075, Dec. 2010.

[6] M. G. D. S. Prado, F. Gardner, M. Damen, and H. Polinder, "Modeling and test results of the Archimedes wave swing," J. Power Energy, vol. 220, no. 8, pp. 855–868, Dec. 2006.

[7] B. Das and B. C. Pal, "Voltage control performance of AWS connected for grid operation," IEEE Trans. Energy Convers., vol. 21, no. 2, pp. 353–361, Jun. 2006.

[8] E. Tara et al., "Dynamic average-value modeling of hybrid-electric vehicular power systems," IEEE Trans. Power Del., vol. 27, no. 1, pp. 430–438, Jan. 2012.

[9] H. L. Do, "Nonisolated bidirectional zero-voltage-switching dc–dc converter," IEEE Trans. Power Electron., vol. 26, no. 9, pp. 2563–2569, Sep. 2011.

[10] D. Salomonsson, L. Söder, and A. Sannino, "An adaptive control system for a dc microgrid for data centers," IEEE Trans. Ind. Appl., vol. 44, no. 6, pp. 1910–1917, Nov./Dec. 2008.